Available online at www.sciencedirect.com
ScienceDirect
Journal of Catalysis 246 (2007) 315–324
JOURNAL OF CATALYSIS
www.elsevier.com/locate/jcat

Stages of aging and deactivation of zeolite LaX in isobutane/2-butene alkylation

Carsten Sievers, Iker Zuazo, Alexander Guzman, Roberta Olindo, Hitrisia Syska, Johannes A. Lercher *

Lehrstuhl II für Technische Chemie, Technische Universität München, Lichtenbergstr. 4, D-85747 Garching, Germany

Received 9 October 2006; revised 7 November 2006; accepted 10 November 2006

Available online 24 January 2007

Dedicated to Prof. Dr. Bernhard Lücke on the occasion of his 70th birthday

Abstract

The formation of carbonaceous deposits and their effect on aging and deactivation of zeolite LaX during isobutane/2-butene alkylation at 348 K were investigated by stopping the reaction at different times on stream. Four stages of the reaction were identified: (1) stable alkylation, (2) deposit transformation, (3) slow deactivation, and (4) rapid deactivation. Deposits consist mostly of bicyclic compounds and branched carbenium ions, which are formed already at the beginning of the reaction and block Brønsted acid sites. During the deposit transformation, migration of smaller entities toward the pore mouth occurs. These cyclic compounds are further alkylated and lead to pore mouth plugging. In the final stage of rapid deactivation, the catalyst stops producing alkylate, and butene oligomerization is the main reaction leading to olefin desorption and massive deposit formation at the outside of the zeolite particles.

Keywords: Alkylation; Isobutane; 2-Butene; Deactivation; Coke; Deposits; Poisoning; Pore mouth plugging; Regeneration; Zeolite

1. Introduction

Isobutane/2-butene alkylation is an important refining process for the production of a complex mixture of branched alkanes, which is an ideal blending component of gasoline. Currently, commercial alkylation processes operate with sulfuric or hydrofluoric acid as catalysts [1]. The acid consumption in the sulfuric acid-based process may reach as high as 70–100 kg/t [2]. The spent sulfuric acid must be worked up in a rather expensive treatment to remove hydrocarbons and water. Hydrofluoric acid, on the other hand, is highly toxic and forms aerosols, making its handling rather difficult. Therefore, many countries no longer allow the building of alkylation units that use HF as catalyst. For this reason, considerable efforts have been made to develop novel alkylation catalysts that are easier to handle and environmentally more friendly [2].

Among the wide variety of solid acids tested as catalysts for isobutane/butene alkylation [3], zeolites have received the most attention. In general, the lifetime of zeolites increases with increasing acid site concentration [4]. In addition, Feller et al. demonstrated that a high ratio Brønsted/Lewis acid sites extends the catalyst lifetime [5]. On the other hand, rapid deactivation was also observed for catalysts with very high Brønsted acidity, e.g., sulfated zirconia [6]. Some speculate that this is linked to the high cracking activity of such materials. Zeolites with a three-dimensional pore structure and large pores show higher time catalytic stability due to a higher diffusivity [7]. The most promising materials tested so far are based on zeolites Beta [4,8,9], X [5,10], and Y [4,11–20].

Despite the potential benefits presented by these catalysts, their industrial application is constrained by rapid deactivation due to the accumulation of carbonaceous deposits. Both poisoning of active sites [14] and pore mouth plugging [12,21] have been proposed as deactivation mechanism.

The main reason for deactivation is that, especially when the alkene concentration is high, addition of an alkene molecule to

* Corresponding author. Fax: +49 89 28913544.
E-mail address: johannes.lercher@ch.tum.de (J.A. Lercher).

0021-9517/$ – see front matter
doi:10.1016/j.jcat.2006.11.015

a carbenium ion is faster than intermolecular hydride transfer. This problem can be partially solved by performing the reaction in a CSTR so that sufficient backmixing is provided and the olefin concentration is kept at a low level in the entire reactor volume [4]. Nevertheless, frequent regeneration steps are needed to extend the total lifetime of a given catalyst to an acceptable length. The patent literature suggests that as many as several hundred regenerations are needed to make processes based on solid catalysts competitive with existing processes using H_2SO_4 and HF [22]. Various regeneration procedures, including extraction with supercritical fluids [19,23,24], combustion [12], and hydrogenative regeneration [25], have been published.

In this respect, a detailed knowledge of the product distribution and formation of carbonaceous deposits with time-on-stream (TOS) is mandatory for understanding the deactivation mechanism(s) and thus designing stable catalysts and efficient regeneration procedures. Various researchers have investigated the deactivation process using a combination of characterization techniques, including IR [10,18,26], UV/vis [7,14,25–27], ^{13}C NMR [14,15,28], and ^{1}H NMR spectroscopy [18,26], as well as temperature-programmed oxidation [12] and matrix-assisted laser desorption ionization-time of flight mass spectrometry (MALDI-TOF MS) [26]. However, the alkylation reaction was often carried out in fixed-bed or batch reactors [7,8,11,12,14,18,19,28–32], in which the catalysts were exposed to high olefin concentrations and thus deactivated within minutes. In addition, only few studies have investigated spent catalysts that had not passed the stage of full olefin conversion [18,25,26]. However, because the number of data points was limited, no detailed time resolved-picture was obtained.

In this paper, we report a multitechnique study on the deactivation of zeolite LaX in isobutane/2-butene alkylation. In previous studies, it was shown that this catalyst has one of the longest lifetimes among the zeolites [5], due to the high Brønsted/Lewis acid site ratio. The alkylation reaction was performed in a CSTR under optimized condition [5]. Deactivation was studied by stopping the reaction after different times on stream, providing a time-resolved picture of the physicochemical properties of the catalyst, in contrast to previous studies, which investigated catalysts after extended use.

2. Experimental

2.1. Catalyst preparation

La-exchanged zeolite X (LaX) was prepared from NaX (Si/Al = 1.2), which was provided by Chemische Werke Bad Köstritz. The parent material was ion exchanged twice in an excess of 0.2 M $La(NO_3)_3$ solution for 2 h at 353 K. The zeolite was thoroughly washed with bi-distilled water and dried at room temperature. Finally, the sample was calcined in air flow with a slow temperature ramp up to 723 K. After rehydration in air, three additional ion-exchange steps, followed by washing, drying, calcination, and rehydration, were performed.

2.2. Catalytic reactions

The alkylation reactions were performed in a CSTR. Before the reaction, the catalyst was activated in situ at 453 K for 14 h in H_2. The reactor was then cooled to 348 K, pressurized to 20 bar, and filled with pure isobutane (AIR LIQUIDE, 99.95%). The reaction was started by feeding a mixture isobutane/2-butene (Messer, 99.4%) with a molar ratio of 10/1. The olefin space velocity was 0.2 $g_{butene}\, g_{catalyst}^{-1}\, h^{-1}$, and the stirring rate was 1600 rpm. The products were analyzed with a HP 6830 gas chromatograph equipped with an flame ionization detector and a 50-m DB-1 column. The products were collected, and isobutane was evaporated after reaction. The remaining organic phase was analyzed by ^{1}H NMR spectroscopy on a Bruker AM 360 spectrometer using $CDCl_3$ as a solvent.

To study the deactivation over time on stream, several catalytic experiments were performed and stopped after different times on stream (0.5, 1.9, 3.8, 5.7, 7.6, 9.5, 12.7, 15.8 h). After drying in nitrogen flow for 4 h at 348 K, the catalyst was removed from the reactor and stored under nitrogen.

2.3. Catalyst characterization

To determine the concentrations of Si, Al, and Na by atomic adsorption spectroscopy (AAS), 20–40 mg of each sample was dissolved in 0.5 ml of hydrofluoric acid (48%) and heated to 343 K until all of the liquid evaporated. The lanthanum content was determined by EDX (Jeol JSM-5900 LV spectrometer). For these measurements, the sample was placed on a conductive carbon target. The spectrometer was operated at a voltage of 25 kV. The measurements were performed on a UNICAM 939 atomic absorption spectrometer. The carbon content of spent catalysts was measured by combustion analysis using an Elementar Vario EL analyzer.

The BET surface area, micropore volume, and pore size distribution of the catalyst were determined by nitrogen physisorption on a PMI Automated BET Sorptometer. Before the measurements, the samples were heated to 393 K for 2 h in vacuum.

Acid site concentrations were obtained from IR spectra of adsorbed pyridine. Before measurement, the samples were pressed into self-supporting wafers and dried under vacuum at 373 K for 2 h to remove water and weakly adsorbed deposits. Such molecules are supposed to have a negligible influence on the catalyst deactivation. Pyridine was adsorbed at 373 K with a pressure of 0.1 mbar until no changes were observed in the spectrum. After outgassing for 1 h to remove weakly physisorbed pyridine, a spectrum was recorded. For quantification, the molar extinction coefficients published by Emeis were used [33].

For MAS NMR measurements, the samples were packed into a ZrO_2 rotor and spun at 15 kHz. The measurements were performed on a Bruker AV500 spectrometer with resonance frequencies of 125.8 MHz for ^{13}C and 130.3 MHz for ^{27}Al. For ^{13}C MAS NMR, the sensitivity was enhanced by applying cross-polarization [34]. The contact time was 5 ms. At least 40,000 scans were recorded for each spectrum. The spectra

were calibrated using the methine carbon atoms of adamantane as an external standard ($\delta = 29.47$ ppm). The ^{27}Al spectra were measured as the sum of 2400 scans with a recycle time of 250 ms. A $\pi/12$ pulse was applied for excitation. The ^{27}Al DOR-NMR measurements were performed on a Bruker AV750 with an outer spinning rate of 1300 Hz and an inner spinning rate of approximately 6 kHz. The resonance frequency for ^{27}Al was 195.5 MHz.

UV/vis spectra were measured on a MCS 320 Zeiss spectrometer in the wavelength region of 190–500 nm. The results are reported as difference spectra, obtained by subtracting the spectrum of the fresh LaX zeolite.

For MALDI-TOF MS, 10 mg of the deactivated catalyst was suspended in 200 µl of a 1% trifluoroacetic acid solution that was saturated with 2,5-dihydroxybenzoic acid (DHB). The mixture was placed in an ultrasonic bath for 15 min. From this suspension 2 µl were deposited onto a sample holder. The samples were dried overnight at room temperature. MALDI-TOF mass spectra were recorded using a Bruker Biflex III MALDI-TOF mass spectrometer equipped with a N_2 laser ($\nu = 337$ nm) operating at a pulse rate of 3 Hz. The ions were accelerated with pulsed-ion extraction after a delay of 50 ns at a voltage of 28.5 kV. The analyzer was operated in reflection mode, and the ions were detected using a microchannel-plate detector. Before measurement, the mass spectrometer was calibrated with a polystyrene standard.

For the analysis of carbonaceous deposits, the spent catalyst was dissolved in 40% HF solution. Excess HF was evaporated, and the residue was extracted with CH_2Cl_2. Carbonaceous deposits formed from reaction at low temperatures have been claimed to be completely soluble in organic solvents [18] and to remain unaltered after the treatment with hydrofluoric acid [35,36]. A Finnigan MAT 8200-GC-MS with a nonpolar OV1 methylpolysiloxane column was used for the measurements. The detector was a II-MS with energy of 70 eV. A 1-µl portion of the extracted sample was injected into the column at room temperature according to the "on-column" method. The temperature was first increased to 343 K for 3 min and then to 633 K (heating rate, 10 K/min) for 15 min.

For additional measurements, the extracts were hydrogenated over night (10 bar H_2, 298 K) using 6 mg of PtO_2. Pater et al. demonstrated that 2,3-dimethyl-2-butene is quantitatively hydrogenated under similar conditions [18].

3. Results

3.1. Characterization of the fresh catalyst

The overall chemical analysis indicated a Si/Al ratio of 1.1. The concentrations of sodium and lanthanum were 0.2 and 23.0 wt%, respectively. The apparent BET surface was 529 m^2/g, and the micropore volume was 0.148 cm^3/g. The pore size distribution indicated that mesopores were formed during catalyst preparation. The total concentrations of Brønsted and Lewis acid sites were 0.47 and 0.14 mmol/g, respectively. The concentrations of strong Brønsted and Lewis acid sites (pyridine molecules persisting evacuation at 723 K) were 0.018 and 0.037 mmol/g, respectively.

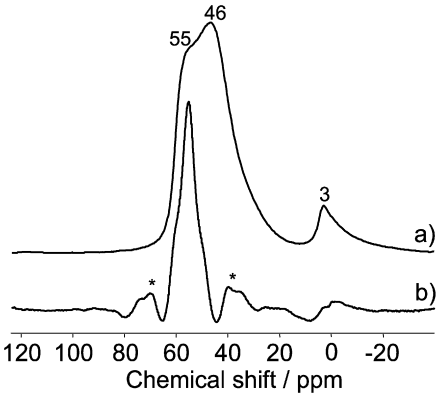

Fig. 1. ^{27}Al MAS NMR spectra of hydrated LaX: (a) ^{27}Al MAS NMR, (b) ^{27}Al DOR NMR. Spinning side bands are marked with ⋆.

The ^{27}Al NMR spectra are shown in Fig. 1. The overlapping peaks at 55 and 46 in the MAS spectrum (Fig. 1a) correspond to aluminum nuclei with tetrahedral coordination. The former peak is assigned to Al with a proton, the latter with La^{3+} as a charge compensation cation [37]. The ^{27}Al double-rotation (DOR) NMR spectrum (Fig. 1b) showed only one peak in this region, indicating that the upfield shift of the second peak was caused by quadrupolar interaction due to a strong distortion of the local environment by the lanthanum cation. It is concluded that charge compensation by La^{3+} does not alter the partial charge of the adjacent Al atoms significantly, but does change the geometry of their coordination sphere. The signal at 3 ppm is assigned to octahedral Al, which is present in the form of an aluminum oxo-cluster or in a separate phase outside the zeolite pores [37,38]. In this region, both spectra have approximately the same line shape, indicating that various chemically different octahedral Al species were present in LaX. Approximately 11% of the Al atoms are in an octahedral environment. Together with the observation of mesopores, this indicates that dealumination has occurred to a certain extent during ion exchange and calcination.

3.2. Catalytic experiments

In the beginning of the reaction, complete conversion of 2-butene was observed (Fig. 2). After 9.5 h, the conversion dropped below 99%, but it decreased slowly. Rapid deactivation started after 12.9 h. Hereinafter, this point is referred to as the end of the catalyst lifetime.

The integral product yield per weight of catalyst is shown in Fig. 3. During the catalyst lifetime, the product mixture is dominated by the C_8 fraction, which is formed at a constant rate, as indicated by the linear increase of the yield with time on stream (TOS) (Fig. 3). The production of octanes stopped within 2 h after the end of the catalyst lifetime. The same trend was observed for the C_5–C_7 fraction, resulting from cracking of large carbenium ions (C_{12} or larger) [5]. The production of heavy products (more than 9 carbon atoms) accelerated somewhat af-

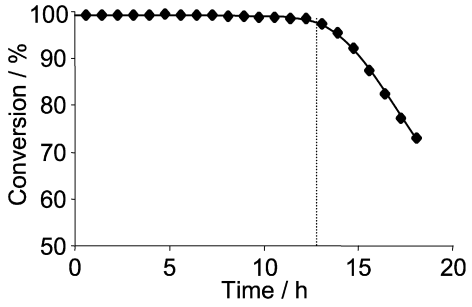

Fig. 2. Conversion of butene during alkylation over LaX at 348 K.

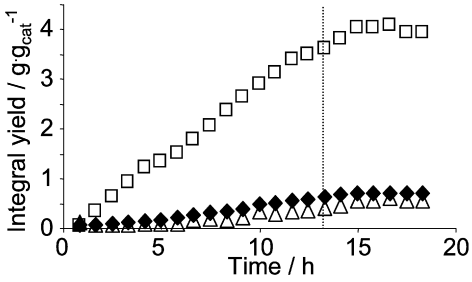

Fig. 3. Integral product group yield during alkylation over LaX at 348 K: (◆) C_5–C_7, (□) C_8, (△) C_{9+}.

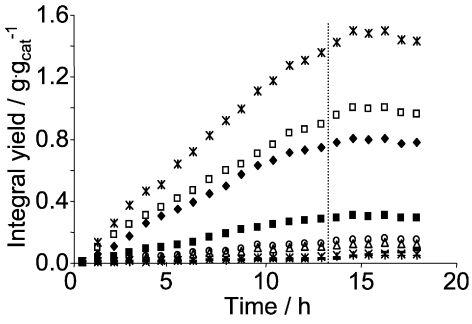

Fig. 4. Integral yield of octane and octene isomers during alkylation over LaX at 348 K: (✱) 2,3,3-TMP, (□) 2,3,4-TMP, (◆) 2,2,4-TMP, (■) 2,5-DMH/2,2,3-TMP, (○) 2,3-DMH, (△) 2,4-DMH, (×) 3,4-DMH, (– –) octene isomers.

ter 6 h TOS and continued for at least 3 h after the end of the catalyst lifetime.

The C_8 fraction consists mainly of trimethylpentane isomers (Fig. 4). Note that only small amounts of 2,2,3-trimethylpentane—the primary product of the addition of butene to a *tert*-butyl carbenium ion—were formed. This indicates that isomerization by methyl group shift is significantly faster than hydride transfer. Feller et al. explained that steric hindrance by the *tert*-butyl group makes hydride transfer to the corresponding carbenium ion unfavorable [5]. Fig. 4 shows that the production of most C_8 products was constant and stopped within 2 h after the end of the lifetime.

A different trend was observed for octene isomers (Fig. 5). During the catalyst lifetime, the C_8 fraction contained at best 0.5 wt% of olefins. This concentration increased drastically after the end of the catalyst lifetime, indicating that at this stage, dimerization of butene was the dominant reaction, whereas the alkylation activity of the catalyst had ceased completely.

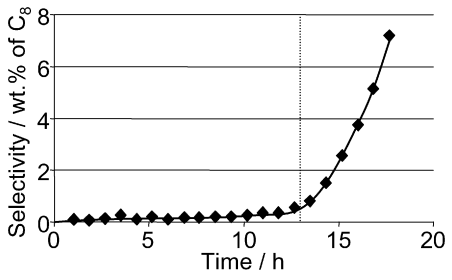

Fig. 5. Selectivity to olefins within the C_8 fraction.

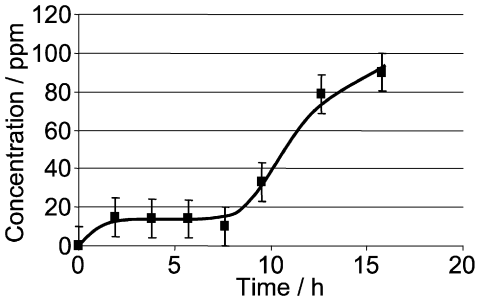

Fig. 6. Concentration of aromatic protons in the alkylate collected during alkylation over LaX at 348 K (measured by ^{1}H NMR).

A more detailed study on product distribution has been published elsewhere [5].

The concentration of aromatics in the product stream was investigated by ^{1}H NMR (Fig. 6). For the first 7.6 h on stream, the concentration of aromatic protons was constant at approximately 15 ppm. Subsequently, a strong increase was observed. Note that these concentrations are integral values. Therefore, the increase in selectivity toward aromatic products is more pronounced than it appears from Fig. 6.

3.3. Characterization of spent catalysts

Fig. 7 shows the carbon content of the catalyst as a function of TOS. In the first 1.9 h, the carbon content increased to a value of approximately 5.5 wt%. This loading remained constant until 9.5 h on stream, then increased again, reaching a value of 10.0 wt% after 15.8 h.

As shown in Fig. 7, in the first 1.9 h on stream, the micropore volume decreased to slightly more than half of the original value and stabilized at this level. After 7.6 h, the micropore volume decreased again until complete blockage of the micropores was observed after 15.8 h.

The concentrations of Brønsted and Lewis acid sites were determined by IR spectroscopy of adsorbed pyridine (Fig. 8). In the first 1.9 h of the reaction, the concentration of Brønsted acid sites available to adsorb pyridine decreased to approximately half of the initial value. However, only a small decrease in the Lewis acid site concentration was observed during this period. Between 1.9 and 5.7 h on stream, the concentrations of Brønsted and Lewis acid sites remained unchanged. This period was followed by a decrease in the concentration of accessible Brønsted and Lewis acid sites between 5.7 and 9.5 h on stream. At this point, both concentrations were reduced to approximately

half of their previous values, after which they remained constant.

The nature of the deposits was investigated by ^{13}C MAS NMR spectroscopy. Cross-polarization was used to obtain spectra with an acceptable signal-to-noise ratio. This pulse sequence does not give quantitative results. In particular, the concentration of aromatic species is underestimated. However, cross polarization can be used to estimate the order of magnitude of a given signal [34,39]. Fig. 9 shows the ^{13}C NMR spectra of LaX after various TOS. In agreement with the trends of the elemental analysis, only a very small increase in overall intensity was observed between 3.8 and 9.5 h. In all samples, most of the carbon atoms were found to be aliphatic. The peak position in the spectra between 3.8 and 9.5 h are identical. They are assigned to methyl groups at secondary carbon atoms (9 and 15 ppm), methyl groups at aromatic carbon atoms (18 ppm), methylene groups bound to methyl groups (23 ppm), and methylene groups in different paraffinic environments or methyl groups bound to quaternary carbon atoms (30 ppm) [28]. The relative intensity of the peak at 18 ppm (CH_3-ar) increased with TOS. In addition to these peaks, a shoulder was observed at 21 ppm, assigned to methyl groups bound to olefinic carbon atoms.

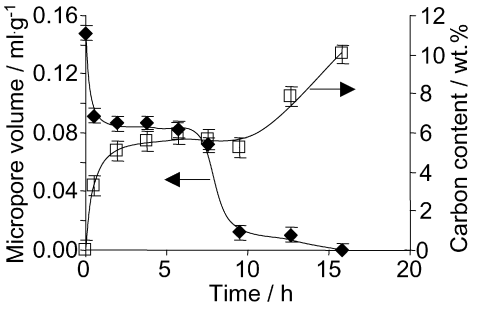

Fig. 7. Carbon content (□, measured by combustion analysis) and micropore volume (◆, determined by N_2 adsorption) of LaX after alkylation.

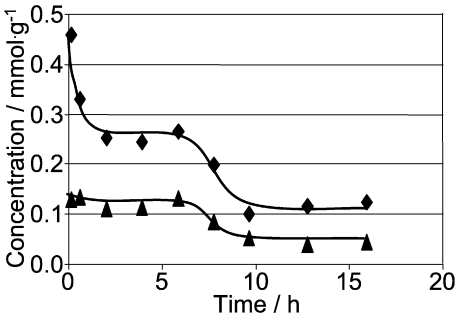

Fig. 8. Concentration of free acid sites on LaX vs TOS (measured by IR spectroscopy of adsorbed pyridine): (◆) Brønsted acid sites, (▲) Lewis acid sites.

Between 9.5 and 15.8 h, the intensity of the ^{13}C NMR signal increased sharply. In the spectrum corresponding to 15.8 h, the peak were shifted by up to 1 ppm. The peak at 9 ppm was observed only as a weak shoulder. In addition, the shoulder at 21 ppm became more pronounced, and an additional shoulder was observed at 32 ppm, which is assigned to methylene groups in paraffinic environment. The increased intensity of the paraffinic bands was due mainly to increases in the secondary and tertiary carbon species (25–50 ppm), whereas the peaks of the different methyl groups increased more moderately. This is speculatively explained by the formation of naphthenic compounds.

In addition to the paraffinic peaks, a broad peak between 105 and 160 ppm was observed in all spectra. This peak is assigned to unsaturated carbon atoms of olefinic or aromatic compounds; its maximum was at approximately 135 pmm. Weitkamp and

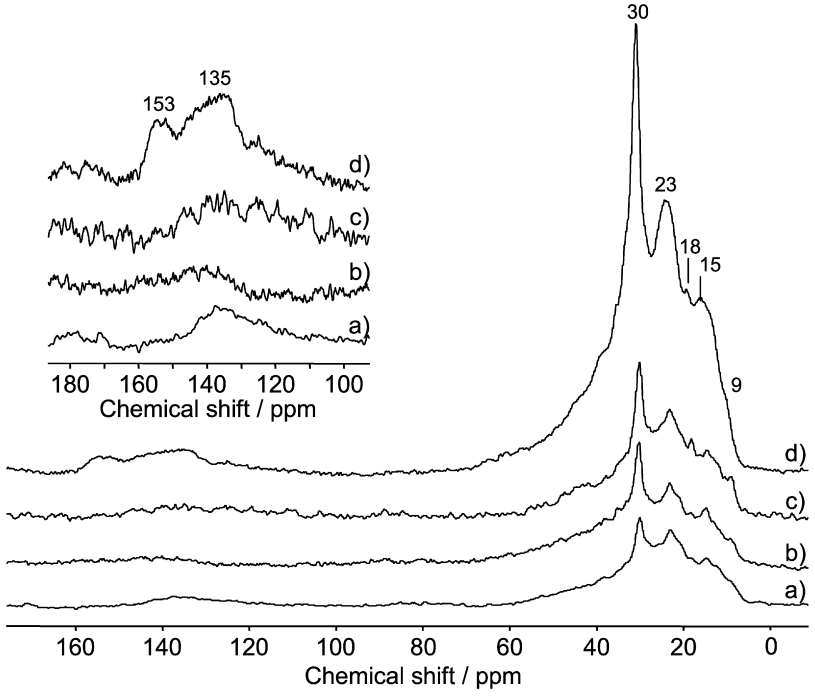

Fig. 9. ^{13}C CP MAS NMR spectra of spent LaX catalysts after alkylation at 348 K for (a) 3.8 h, (b) 7.6 h, (c) 9.5 h, and (d) 15.8 h.

Maixner suggested to assign a peak in this position to substituted or bridged aromatics or olefins [28]. Due to the low concentration of aromatics in the product stream, this peak more likely corresponds to olefinic carbon atoms. In the spectrum after 15.8 h on stream, an additional peak at 153 ppm was observed. We tentatively assign this peak to highly substituted aromatic ring systems. Alternatively, the signal could be attributed to oxygen-containing unsaturated species. In all NMR spectra, the area of the peaks corresponding to unsaturated carbon atoms was approximately 8% of the total integral of the individual NMR spectrum. Note that the concentration of unsaturated carbon species may be underestimated because of the CP pulse sequence.

The unsaturated deposits on the catalyst were further investigated by solid-state UV/vis spectroscopy (Fig. 10). The band at the lowest wavenumber is assigned to monoenyl carbocations [40]. The position of this band shifted from approximately 300 nm for the first samples to 315 nm for the samples after 12.7 and 15.8 h on stream. The band at 380 nm is assigned to dienyl carbocations; its position varied only slightly. At 470 nm, a weak band was observed, assigned to trienyl carbocations.

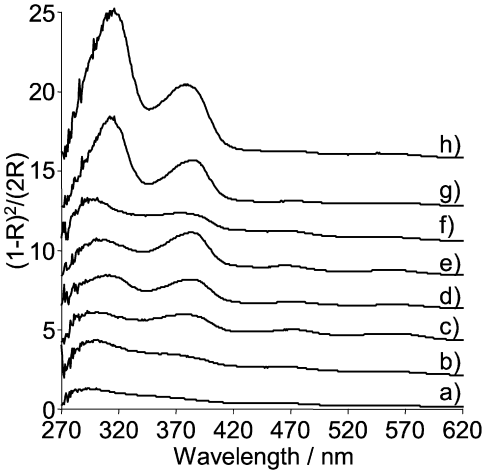

Fig. 10. Solid state UV–vis spectra of the spent LaX catalysts after alkylation for (a) 0.5 h, (b) 1.9 h, (c) 3.8 h, (d) 5.7 h, (e) 7.6 h, (f) 9.5 h, (g) 12.7 h, and (h) 15.8 h.

In the two spectra recorded at short TOS (0.5 and 1.9 h), only the monoenyl band is well resolved. Between 3.8 and 9.5 h TOS, all three bands were observed with some fluctuation of the relative intensities. A strong increase was observed for the monoenyl carbocation peaks after 12.7 h on stream, whereas the trienyl band was no longer observed. In the last spectrum, the bands of monoenyl and dienyl carbocation increased strongly, indicating that the formation of unsaturated deposits by dehydrogenation becomes a significant reaction pathway only at the end of the catalyst lifetime.

The spent catalysts were also characterized by MALDI-TOF MS, which was previously applied to spent FCC [41,42] and alkylation [26] catalysts. This method can detect protonated or cationized (i.e., addition of Na^+ or K^+) species. The main drawback of MALDI-TOF MS is that heteronuclear and unsaturated compounds are ionized significantly easier than saturated hydrocarbons [26,43]; therefore, the spectra may represent minority species.

Fig. 11 shows the MALDI-TOF mass spectra of the LaX catalysts after different TOS, in good agreement with previous results [26]. The spectra are dominated by a sequence of peaks that differ by 14 m/z. This difference corresponds to the addition of a CH_2 groups, that is, the extension of an alkyl chain by one carbon atom or the replacement of a proton by a methyl group. Every forth peak in this series was more pronounced. The smallest mass in this series was 137 m/z. Based on the assumption that protonated species are detected, this peak corresponds to the empirical formula $C_{10}H_{16}$ or $C_9H_{12}O$. In addition to the main series, two parallel series were observed, which were shifted by 2 m/z units to lower masses and by 1 m/z unit to higher masses with respect to the main series. The first series corresponds to compounds with an additional double bond, whereas the second series is tentatively assigned to molecules

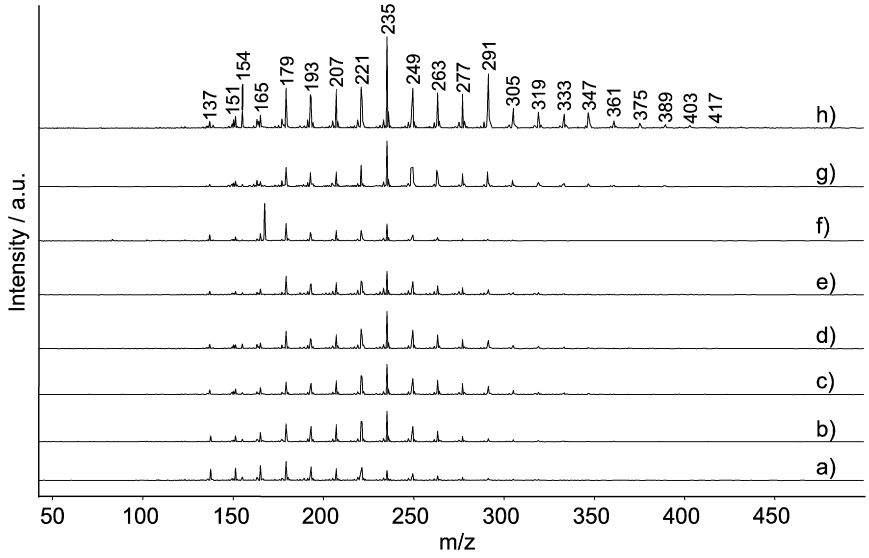

Fig. 11. MALDI-TOF mass spectra of spent LaX after (a) 0.5 h, (b) 1.9 h, (c) 3.8 h, (d) 5.7 h, (e) 7.6 h, (f) 9.5 h, (g) 12.7 h, and (h) 15.8 h.

that were ionized by loss of an electron, thus having a mass higher (by 2 m/z) than the main series.

Only a weak matrix peak (DHB + H^+) at 155 m/z was observed. Attenuation of this feature is generally associated with readily ionizable heterocompounds [44]. From this observation, Feller et al. proposed that oxygenated compounds are formed during alkylation at 348 K [26]; however, we cannot exclude their formation during sample preparation for MALDI-TOF MS measurement.

Few differences were found in the intensities of the spectra up to 9.5 h on stream. Only the peaks corresponding to higher masses in the spectrum after 0.5 h were somewhat smaller than in the following spectra. After 12.7 h, a small increase was observed; after 15.8 h, the intensities of all peaks strongly increased. At the same time, the highest observed mass increased from 361 m/z after 9.5 h to 501 m/z after 15.8 h.

For further investigation of the deposits, the spent catalysts were decomposed in HF. The carbonaceous deposits were extracted from the residue with CH_2Cl_2 and analyzed by GC/MS. In agreement with previous studies on USHY, it was found that the most abundant compounds had a composition of C_nH_{2n-4}, indicating that they contain three double bonds or aromatic rings [18,20]. Compounds with composition C_nH_{2n-2} and C_nH_{2n-6} were also detected. The majority of the deposits had a carbon number in multiples of 4. In all mass spectra, strong peaks were observed for 43 and 57 m/z, indicating that the corresponding molecules contained alkyl chains.

A part of the extracted phase was hydrogenated to differentiate between double bonds and cycles in the deposit molecules. After hydrogenation, the composition C_nH_{2n-2} was dominant. This indicates that most of the deposits are bicyclic molecules with one double bond [18]. Saturated compounds and molecules with two double bonds were observed in lower concentrations. Compounds with 9–40 carbon atoms were detected. The most abundant species had 24–32 carbon atoms. The complexity of the mixture precluded precise quantification of the chromatograms, however.

4. Discussion

4.1. Modification of the catalytic properties

Deactivation of zeolite-based catalysts in isobutane/2-butene alkylation has been the subject of several studies. However, there is still a dispute about the extent to which poisoning of active sites [14] and pore mouth plugging [12,21] contribute to catalyst deactivation. Several papers suggest that both routes contribute [25,26,45]. In this scenario, deposits adsorb irreversibly on Brønsted acid sites, thereby decreasing the concentration of active sites for alkylation. As the concentration of acid sites decreases, the nominal severity (mol butene feed/time and Brønsted acid site) increases. As with a formal increase of the severity, this results in a faster deactivation of the catalyst. Note that the turnover per site increases in this scenario as the concentration decreases. Separate measurements have shown that this results in a lower product quality (i.e., less pronounced hydride transfer) and a shorter absolute usable lifetime [5]. As a result, polymerization begins to dominate over alkylation. In turn, the formed polymers cause pore mouth plugging. However, these speculations have not been supported by measurements of the concentration of accessible Brønsted acid sites as a function of TOS.

Most previous studies have investigated catalysts that had already passed the stage of full olefin conversion [7,10–12,14,45,46]. This approach does not allow differentiation between modifications of the catalyst that cause deactivation and those occurring after the catalyst has lost its alkylation activity. To obtain a comprehensive model of the deactivation process, the present study focuses on the characterization of used LaX catalyst after different times on stream.

Based on the product distribution and characterization of the spent catalysts, the alkylation of isobutane with 2-butene over LaX is divided into four stages: (1) stable alkylation, (2) deposit modification, (3) slow deactivation, and (4) rapid deactivation. At the beginning of the first stage, stable alkylation, carbenium ions are formed by protonation of 2-butene molecules. Note that the ground state of the surface species also may be described as alkoxy groups; however, their conversion is appropriately described as carbenium ion chemistry. Therefore, here we call them carbenium ions. Adding olefins to the carbenium ions leads to the formation of octyl, dodecyl, and hexadecyl carbenium ions. These reactions result in increased carbon content and decreased of the micropore volume and Brønsted acid site concentration. Under the experimental conditions used here, steady-state is reached after 1.9 h on stream. At this point, the carbon content is 5.5 wt%, which would correspond to nearly 50% micropore filling with isooctane using its liquid-phase density. Note that this corresponds qualitatively to the measured decrease of the micropore volume using nitrogen adsorption. This situation remains stable until 5.7 h on stream.

In the second stage between 5.7 and 9.5 h on stream, changes in the nature of the deposit must occur while still ensuring complete conversion of 2-butene. As the concentrations of Brønsted and Lewis acid sites decrease, the total carbon content remains unchanged. This suggests that the chemisorbed species are smaller in nature but better distributed throughout the material. In the last stage of this phase, a drastic decrease of the micropore volume from 0.07 to 0.01 ml/g is observed, again without changes in carbon content (see Fig. 12). Thus, the deposit transforms further and/or migrates to the pore mouths, blocking the entrance for nitrogen. As discussed in detail below, significant modifications of the chemical composition of the deposits are not observed at this stage. Therefore, we conclude that bulky deposits block an increasing part of the pore volume.

The stage of slow deactivation starts after 9.5 h on stream, when the 2-butene conversion drops below 99% and decreases slowly but steadily. At the same time, the carbon content increases significantly. Because the pores were already half-filled in the first two phases, this increase is attributed mainly to the formation of deposits outside of the pores. Completion of micropore blocking is slow due to the three-dimensional nature of the faujasite lattice. Despite the drastic decrease in pore volume in this stage, most of the 2-butene entering the reactor is still

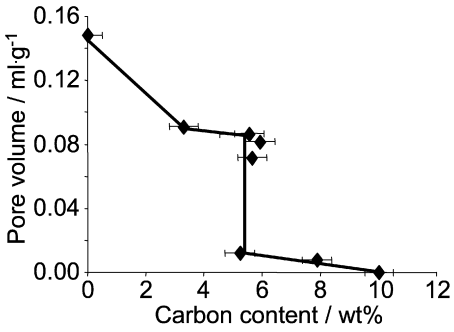

Fig. 12. Correlation between micropore volume and the carbon content during isobutane/2-butene alkylation over LaX.

converted, and the product stream is still dominated by alkylation products. Therefore, the reaction is speculated to occur at a limited number of active sites close to the pore mouths.

After 12.9 h, the stage of rapid deactivation starts. Polymerization at the outside of the zeolite particles leads to a drastic increase in the carbon content. This is also demonstrated by the increased concentration of octene isomers in the product stream, which result from the dimerization of 2-butene. The formation of deposits outside the zeolite pores completes the pore mouth plugging. In agreement with previous results, the micropores of LaX are completely blocked at this stage, but some of the deposits can still be replaced by pyridine [26]. Note that in this context, a key role of pore mouth plugging was also suggested in a modeling study by Sahebdelfar et al. [21], indicating that pore mouth plugging is essential to explaining the changes of the conversion over time.

4.2. Nature of the deposits

In agreement with previous studies, we observed that the majority of the carbon atoms are aliphatic [14,15,18,28]. However, it must be kept in mind that cross-polarization (CP) NMR underestimates carbon atoms, which are not bound to hydrogen atoms [34]. The peak of unsaturated carbon atoms amounted to 8% of the total intensity; this value is equivalent to 1 double bond per 25 carbon atoms. Note that this ratio remained constant over TOS. The total intensity of the spectrum was in good agreement with the combustion analysis, increasing only slightly between 3.8 and 9.5 h on stream and more strongly when the reaction proceeded further.

Despite the high concentration of saturated carbon atoms, it has been suggested that unsaturated compounds play a key role in the deactivation process [14,25]. This may be the case if a minority species irreversibly blocks the active sites of the catalyst. Various studies have investigated deactivated zeolitic alkylation catalysts by UV–vis spectroscopy [14,25,26]. In all of these studies, enylic carbocations were observed on the used catalysts and proposed to be strongly adsorbed on Brønsted acid sites. In the present study, the bands of enylic cations modestly increased during the initial stage of the reaction, but a stronger increase was observed only after the end of the catalyst lifetime. This indicates that enylic cations are already formed at the beginning of the reaction. It is interesting to note that the band

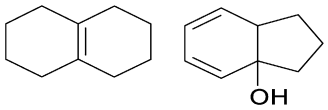

(a) (b)

Scheme 1. Possible deposit molecules with a molecular mass of 136 m/z: (a) $C_{10}H_{16}$, (b) $C_9H_{12}O$.

of monoenylic cations remained constant after 1.9 h, wheres the band of bienylic cations still increased and remained constant only after 3.8 h. Afterward, the UV–vis bands did not change dramatically until 12.7 h on stream. The initial increase in concentration of enylic cations coincides with the decrease in strong acid sites. However, through the further transformation, it appears that this may be at least in part a parallel process. We speculate that the zeolite catalyzes a slow dehydrogenation of the surface species through direct dehydrogenation [14], as well as repeated hydride transfer steps [26].

Only a few studies have suggested specific molecular structures for these deposits [7,18]. Yoo et al. identified various saturated and unsaturated cyclic structures for different zeolites [7]. Pater et al. investigated extracted deposits after alkylation over USHY by GC–MS and found bicyclic systems with one double bond as the dominant species [18]. Using the same approach, we detected bicyclic compounds with 0, 1, or 2 double bonds. When a bicyclic molecule is protonated on a Brønsted acid site a tertiary carbenium ion will be the preferred product. Hydride transfer from an isobutane molecule to this carbenium ion will experience severe steric hindrance, particularly when alkyl side chains are attached to the bicyclic system. Therefore, bicyclic compounds can efficiently block Brønsted acid sites. We assume that spontaneous desorption/deprotonation may be the more likely pathway for removing a bicyclic carbenium ion from a Brønsted acid site, allowing migration of a different site.

The smallest masses found by GC mass analysis correspond to compounds with 9 carbon atoms. However, compounds with a retention time similar to the solvent (CH_2Cl_2) may not be detected using this approach. This drawback was avoided with the MALDI-TOF MS measurements, in which the spent catalyst is only mixed with the matrix and deposited on the target. The smallest molecules detected by MALDI-TOF MS had the sum formula $C_{10}H_{16}$ or $C_9H_{12}O$. Possible molecular structures are shown in Scheme 1. The sensitivity of bicyclo-decene (Scheme 1a) is expected to be rather low, because this molecule will lose its only π-system by protonation. Bicyclo-nona-dienol (Scheme 1b), on the other hand, maintains a double bond when protonated and contains an oxygen atom, further enhancing its sensitivity in the MALDI-TOF MS experiments. Moreover, the suppression of the matrix peak is an indication for molecules containing hetero atoms [26,44]. Therefore, it is reasonable to assume that $C_9H_{12}O$ is the correct empirical formula for the lowest mass peak in the MALDI-TOF mass spectra. This is confirmed by the observations from the GC–MS measurements where bicyclic compounds with 9 carbon atoms were also observed as the smallest molecules. The presence of oxygen in the deposit molecule, however, is attributed to an artifact resulting from a chemical process during pretreatment of the spent catalysts trifluoroacetic acid solution. The absence of alkenes in the

MALDI-TOF MS is attributed to the selectivity of the ionization process [43].

The periodicity in the MALDI-TOF mass spectra indicates that most deposit molecules contain alkyl side chains attached to the bicyclic ring system. These molecules are so bulky that they must be located at the pore mouth or at the outer surface of the zeolite, so that at least parts of them lie outside the microporous network of the zeolite.

The preference toward compounds with carbon numbers that are multiples of 4 indicates that considerable amounts of the deposits are formed by oligomerization of butene without being affected by cracking. This observation is in apparent contrast to the fact that the concentration of C_5–C_7 products was 8–15 wt%, indicating that cracking of carbenium ions is an important reaction pathway. However, the large deposit molecules discussed above are chemisorbed via the bicyclic system. In that scenario, the formation of C_5–C_7 alkanes involves cracking of the alkyl side chains, including the formation of a di-cation. Because cracking of the saturated side chain would require formation of a carbonium ion or a hydride-transfer step involving very large carbenium ions, we conclude that it is rather unlikely under the reaction conditions used here. This in turn indicates that cracking leading to C_5–C_7 products occurs preferentially via smaller carbenium ions.

The largest detected masses correspond to molecules with 40 carbon atoms, which contain long and bulky alkyl side chains. Because these molecules are readily observed in MALDI-TOF MS measurements, they must be located preferentially near or on the outer surface of the catalyst. We speculate that during the second stage, bicyclic molecules migrate to the pore mouths, where the side chains are added. Because all characterization methods suggest the absence of major changes in the deposits' nature while the catalyst remains active, we conclude that migration of the deposits must play a key role in deactivation by inducing pore mouth plugging.

These results suggest that modifications of the catalysts that ultimately lead to deactivation start after approximately 5.7 h on stream (under the current experimental conditions). For a long-term stable operation of such solid catalysts, regeneration must set in at this point. This regeneration must be very mild; otherwise the cyclic compounds could rapidly dehydrogenate and become very hard to remove.

5. Conclusion

The stages of LaX deactivation during isobutene/2-butene alkylation have been investigated by characterization of the used catalyst after different times on stream. Four stages of the catalyst life have been identified: (1) initiation and stable alkylation, (2) deposit modification, (3) slow deactivation, and (4) rapid deactivation. During the induction period, octyl, dodecyl, and hexadecyl carbenium ions are formed by sorption of *n*-butene on Brønsted acid sites and subsequent alkylation or hydride transfer to isobutane and alkylation with *n*-butene. After this short period, the carbon content remains constant at 5.5 wt% with approximately 50% loading of the total pore capacity until 9.5 h on stream. Over time, the deposit transforms and redistributes into smaller entities, which eventually block most Brønsted acid sites. At this stage, some molecules migrate toward the pore mouth, leading to a significant reduction in the micropore volume by blocking. While this process continues, these molecules are being alkylated, forming larger deposits at the outer surface and pore mouth, more effectively blocking access to the micropores. For a limited time, alkylation is observed on the acid sites, which are still accessible. Olefin addition at the outside of the zeolite increases in importance and leads to rapid accumulation of deposits once the sites for alkylation are not accessible. Most of the deposit molecules are bicyclic systems with one or two double bonds and alkyl side chains. The nature of the deposits does not change significantly during the catalyst lifetime. Significant amounts of aromatic compounds are seen only when deactivation is apparent. This suggests that in addition to these processes, dehydrogenation can occur either via hydrogen elimination from chemisorbed molecules or via multiple hydride transfer steps. To maintain long catalyst life, zeolite catalysts should be regenerated before redistribution of the hydrocarbon sets in.

Acknowledgments

The authors thank Professor Freude and Mr. Schneider for the ^{27}Al DOR NMR measurements, and Mr. Krause for the GC–MS measurements and support for MALDI-TOF MS measurements. They also thank Patrick Magnoux for GC–MS reference measurements. Financial support from Süd-Chemie AG and Lurgi GmbH is gratefully acknowledged. The authors thank Dr. G. Burgfels and Dr. H. Buchold for fruitful discussions. Partial financial support by the European Union in the framework of NMP3-CT-2005-011730 IDECAT WP5 is gratefully acknowledged.

References

[1] L.F. Albright, Ind. Eng. Chem. Res. 42 (2003) 4283.
[2] J. Weitkamp, Y. Traa, Catal. Today 49 (1999) 193.
[3] A. Feller, J.A. Lercher, Adv. Catal. 48 (2004) 229.
[4] K.P. de Jong, C.M.A.M. Mesters, D.G.R. Peferoen, P.T.M. van Brugge, C. de Groot, Chem. Eng. Sci. 51 (1996) 2053.
[5] A. Feller, A. Guzman, I. Zuazo, J.A. Lercher, J. Catal. 224 (2004) 80.
[6] A. Corma, M.I. Juan-Rajadell, J.M. Lopéz-Nieto, A. Martínez, C. Martínez, Appl. Catal. A Gen. 111 (1994) 175.
[7] K. Yoo, E. Burckle, P. Smirniotis, Catal. Lett. 74 (2001) 85.
[8] K. Yoo, P.G. Smirniotis, Appl. Catal. A Gen. 227 (2002) 171.
[9] A. Corma, A. Martínez, P.A. Arroyo, J.L.F. Monteiro, E.F. Sousa-Aguiar, Appl. Catal. A Gen. 142 (1996) 139.
[10] R. Josl, R. Klingmann, Y. Traa, R. Gläser, J. Weitkamp, Catal. Commun. 5 (2004) 239.
[11] Y. Zhuang, F.T.T. Ng, Appl. Catal. A Gen. 190 (2000) 137.
[12] C.A. Querini, E. Roa, Appl. Catal. A Gen. 163 (1997) 199.
[13] A. Corma, A. Martínez, C. Martínez, J. Catal. 146 (1994) 185.
[14] C. Flego, I. Kiricsi, W.O. Parker, M.G. Clerici, Appl. Catal. A Gen. 124 (1995) 107.
[15] M. Stöcker, H. Mostad, T. Rørvik, Catal. Lett. 28 (1994) 203.
[16] T. Rørvik, H. Mostad, O.H. Ellestad, M. Stocker, Appl. Catal. A Gen. 137 (1996) 235.
[17] K.S. Yoo, P.G. Smirniotis, Catal. Lett. 103 (2005) 249.
[18] J. Pater, F. Cardona, C. Canaff, N.S. Gnep, G. Szabo, M. Guisnet, Ind. Eng. Chem. Res. 38 (1999) 3822.

[19] D.M. Ginosar, D.N. Thompson, K.C. Burch, Appl. Catal. A Gen. 262 (2004) 223.
[20] F. Cardona, N.S. Gnep, M. Guisnet, G. Szabo, P. Nascimento, Appl. Catal. A Gen. 128 (1995) 243.
[21] S. Sahebdelfar, M. Kazemeini, F. Khorasheh, A. Badakhshan, Chem. Eng. Sci. 57 (2002) 3611.
[22] J. Weitkamp, Y. Traa, in: G. Ertl, H. Knözinger, J. Weitkamp (Eds.), Handbook of Heterogenous Catalysis, vol. 4, Wiley–VCH, Weinheim, 1997, p. 2039.
[23] D.N. Thompson, D.M. Ginosar, K.C. Burch, Appl. Catal. A Gen. 279 (2005) 109.
[24] D.N. Thompson, D.M. Ginosar, K.C. Burch, D.J. Zalewski, Ind. Eng. Chem. Res. 44 (2005) 4534.
[25] R. Klingmann, R. Josl, Y. Traa, R. Gläser, J. Weitkamp, Appl. Catal. A Gen. 281 (2005) 215.
[26] A. Feller, J.-O. Barth, A. Guzman, I. Zuazo, J.A. Lercher, J. Catal. 220 (2003) 192.
[27] I. Kiricsi, C. Flego, G. Bellussi, Appl. Catal. A Gen. 126 (1995) 401.
[28] J. Weitkamp, S. Maixner, Zeolites 7 (1987) 6.
[29] K. Yoo, P.G. Smirniotis, Appl. Catal. A Gen. 246 (2003) 243.
[30] A. Platon, W.J. Thomson, Appl. Catal. A Gen. 282 (2005) 93.
[31] L.M. Petkovic, D.M. Ginosar, Appl. Catal. A Gen. 275 (2004) 235.
[32] K. Yoo, E.C. Burckle, P.G. Smirniotis, J. Catal. 211 (2002) 6.
[33] C.A. Emeis, J. Catal. 141 (1993) 347.
[34] C.E. Snape, B.J. McGhee, J.M. Andresen, R. Hughes, C.L. Koon, G. Hutchings, Appl. Catal. A Gen. 129 (1995) 125.
[35] P. Magnoux, P. Roger, C. Canaff, V. Fouche, N.S. Gnep, M. Guisnet, Stud. Surf. Sci. Catal. 34 (1987) 317.
[36] M. Guisnet, P. Magnoux, Appl. Catal. A Gen. 212 (2001) 83.
[37] J.A. van Bokhoven, A.L. Roest, D.C. Konigsberger, J.T. Miller, G.H. Nachtegaal, A.P.M. Kentgens, J. Phys. Chem. B 104 (2000) 6743.
[38] S.M.C. Menezes, V.L. Camorim, Y.L. Lam, R.A.S. San Gil, A. Bailly, J.P. Amoureux, Appl. Catal. A Gen. 207 (2001) 367.
[39] C.E. Snape, B.J. McGhee, S.C. Martin, J.M. Andresen, Catal. Today 37 (1997) 285.
[40] H. Förster, J. Seebode, P. Fejes, I. Kiricsi, J. Chem. Soc. Faraday Trans. 83 (1987) 1109.
[41] J.O. Barth, A. Jentys, J.A. Lercher, Ind. Eng. Chem. Res. 43 (2004) 2368.
[42] H.S. Cerqueira, C. Sievers, G. Joly, P. Magnoux, J.A. Lercher, Ind. Eng. Chem. Res. 44 (2005) 2069.
[43] A.W. Ehlers, C.G. de Koster, R.J. Meier, K. Lammertsma, J. Phys. Chem. A 105 (2001) 8691.
[44] R. Knochenmuss, F. Dubois, M.J. Dale, R. Zenobi, Rapid Commun. Mass Spectrom. 10 (1996) 871.
[45] F.A. Diaz-Mendoza, L. Pernett-Bolano, N. Cardona-Martínez, Thermochim. Acta 312 (1998) 47.
[46] C.A. Querini, Catal. Today 62 (2000) 135.